International Journal of Trendy research in Engineering and Technology (IJTRET)
Volume 1 Issue 3 Dec 2017

SOLGEL SYNTHESIS OF SILVER DOPED STRONTIUM HEXAFERRITE NANOPARTICLES

[1]K. Alamelu Mangai , [1]K. Tamizh selvi , [2]M. Priya
[1]Department of Physics, Vel Tech High Tech Dr. Rangarajan Dr. Sakunthala Engineering College, Chennai,
[2]Department of Physics, Saveetha Engineering College, Chennai, India

ABSTRACT

Silver doped $SrFe_{12}O_{19}$ samples were synthesized by solgel method based on decomposition of metal nitrates.The samples were characterized by different structural, and electrical measurements. X-ray diffraction data confirmed hexagonal structure of the samples. From the structural analysis it was found that at high Ag doping level, metallic silver is formed as secondary phase. Dielectric permittivity and dielectric loss found to decreae with increase of Ag doping whereas the conductivity of composites found to increase with increasing the Ag^{1+} content as a function of frequency and temperature.
Keywords:$SrFe_{12}O_{19}$,Solgel technique,Dielectric constant, Tangent loss,Dielectric permittivity

1. INTRODUCTION

In past few years, mixed ferrites have attracted much attention because of their vast applications, ranging from microwave to radio frequencies such as microwave devices, computer memories and magnetic recording [1-5]. Semiconductor technologies are developing magnetic random access memories where non-volatile magnetic dots are used for storage capacities of a traditional semiconductor. The typical grain size is essential in the storage of today's commercial magnetic hard disks [6].

The addition of silver to strontium hexaferrite will provide a new composite material with good magnetic behavior. The influence of magnetic and antibacterial properties can make this material unique for applications in biomedicine. Okasha et al. [7] studied the effect of silver substitution in magnesium ferrite and observed an enhancement in its thermal and electrical conductivity. Sun et al. have shown that the biological activity of Fe_3O_4 nanoparticle which was improved by coating a thin film of silver onto it. Nanoparticles of silver, TiO_2 and ZnO are used as antimicrobials and additives in consumer and industrial products.

In this work the effect of Ag substitution on structural and dielectric $SrAg_xFe_{(12-x)}O_{19}$, (x=0.1, 0.2, 0.3) nanoparticles has been reported.

2. EXPERIMENTAL PROCEDURE

Synthesis of strontium hexaferrites

Silver substituted strontium hexagonal ferrite nano composites $SrAg_xFe_{(12-x)}O_{19}$ with $0.1 \leq x \leq 0.3$ in steps of 0.1 were synthesized by sol-gel technique from mixing the pure nitrates

Received 23 December 2017
Revised 25 December 2017
Accepted 26 December 2017

$(Fe(NO_3)_3.9H_2O$, $Sr(NO_3)_2$, $Ag(NO_3)_2$ in ethylene glycol which acts as a gel precursor. The nitrate salt solutions were stirred completely at optimum temperature until the gel was formed. The gel was allowed for dehydration in the time period of 72 hrs and dried gel was obtained and the as-synthesized powder was calcined at 800 °C for 96 hrs in a temperature programmed furnace. Then the material was allowed to cool naturally and compressed to make pellets in a disc shaped form of 13mm diameter and about 0.5mm – 2.5mm thickness and finally sintered at 800 °C for 2h in order to improve the hardness of the bulk samples. The samples were well polished and coated by silver paste for the electrical conductivity measurements.

3. Methods and Characterization

The powder samples were characterized by using powder x-ray diffractometer (XRD) using CuKα radiation source at room temperature. The data were carefully analyzed and Reitveld method employed with the full-prof program for refinement and determining the structural properties [8]. Electrical conductivity of the investigated samples was measured in a wide range of temperature from the temperature 273K up to 573K in static air using Novo control broadband dielectric spectrometer in the frequency range of 1Hz – 40 MHz over a temperature of 0K – 573K. The ac conductivity, the dielectric constant and the loss tangent tan δ as functions of frequency at different temperatures have been studied in detail.

4. RESULTS AND DISCUSSION

4.1. Structural Analysis

X-ray Diffraction

The XRD patterns of $SrFe_{12-x}Ag_xO_{19}$ ($0 \leq x \leq 0.3$) samples are shown in Figure 1. The peaks of XRD patterns are successfully indexed with M-type hexagonal structure of $SrFe_{12}O_{19}$ (ICSD # 20-2518) belonging to the $P6_3/mmc$ space group. The additional diffraction peaks of metallic silver impurity were also observed. The relative intensities of silver peaks increases with increasing silver content. Different reports confirms the existence of metallic silver impurity as secondary phase in the substitution of the Ag^{1+} in hexaferrite structure (Laurent et al. 2008). Because of the large atomic radius of silver Ag^{1+} (1.26 A˚) thanFe^{3+} (0.64 A˚), the substitution of Ag in Fe site could causes the crystalline deficiencies in the hexaferrite structure and forming the metallic Ag^{1+} ion in the interstitial sites of nanoparticles in which the particle has no regular arrangement of atoms. This results in the formation of slight aggregation of secondary phases on the grain boundaries.

The average crystallite size (D) of the samples was calculated by Debye-Scherrer equation [9] and it was found to be around ~1 nm. This can be attributed to low tendency of Ag entering in to the structure. Because of the crystalline deficiencies in the Ag^{1+} ion substitution in the shell of nanoparticles which prevent the growth of crystallite size.

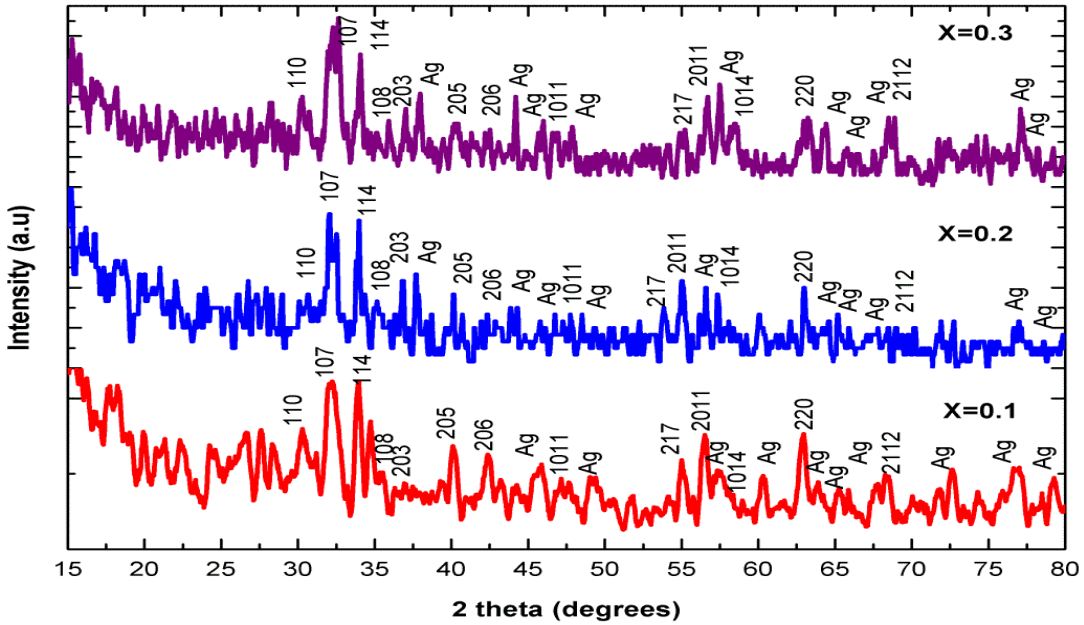

Figure.1. XRD Patterns of $SrFe_{12-x}Ag_xO_{19}$, (x=0.1, 0.2 and 0.3).

4.3. Dielectric Studies

4.3.1. Frequency dependence of Dielectric Properties

Figure 2 (a-c) and 3(a-c) shows the frequency dependence of real and imaginary permittivity of $SrAg_{(1-x)}Fe_{(12-x)}O_{19}$ (x=0.1, 0.2, 0.3) at different temperatures. Complex permittivity (ε=ε'-jε'') represent the dielectric properties of magnetic materials. The real parts of complex permittivity

symbolize the storage capacity of the electric energy. The imaginary part ε'' represent the loss of electric energy. It is worth noting that the real and imaginary dielectric constant decreases with increase of frequency which is the normal behavior observed in hexagonal ferrites. This behavior of dielectric constant with frequency can be explained by Koop's theory which describes the inhomogeneous dielectric medium with two Maxwell and Wagner type layers [10].According to this model, the dielectric material composed of the highly conducting grains separated by the low conducting grains boundaries.

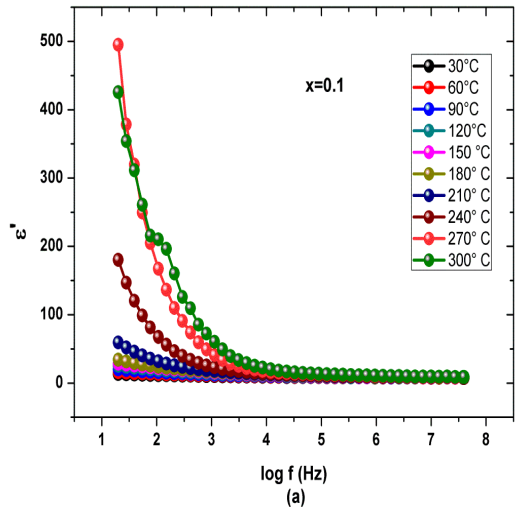

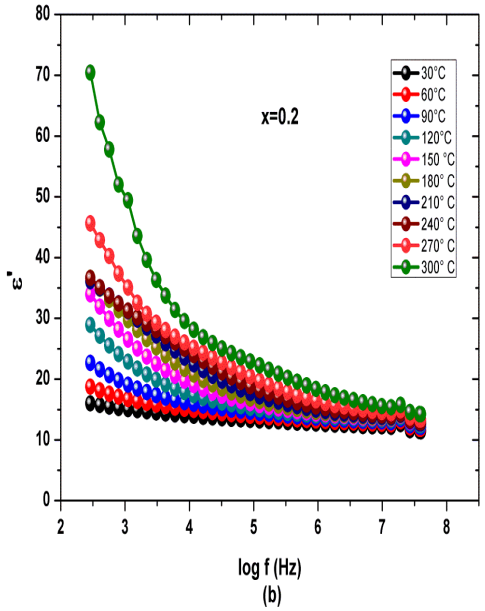

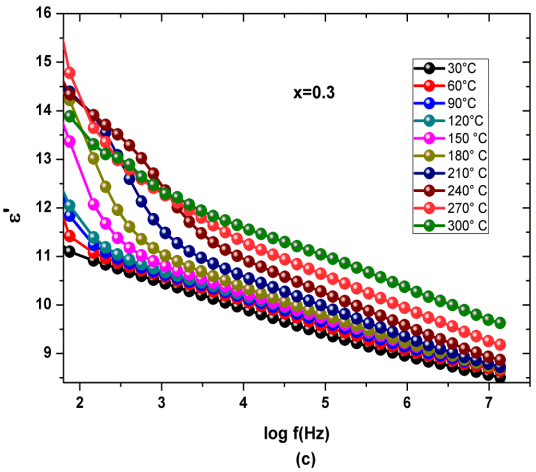

Figure.2 (a-c) Variation of real part of dielectric permittivity (ε') with frequency of $SrFe_{12-x}Ag_xO_{19}$ (x=0.1, 0.2, 0.3) at different temperatures

Rezlescue model [11] stated that the dielectric polarization mechanism in ferrites is related to the conduction mechanism. The ferrites conducting grains are more effective on high frequency regime and poorly conducting grains boundaries play a major role on low frequencies which responsible for high dielectric constant at low frequencies. The reduction of ε' value at higher frequency occurs because beyond a certain frequency, the electronic exchange between ferrous and ferric ions, i.e., Fe^{2+} - Fe^{3+}, cannot follow the alternating field. The large value of ε' at lower frequencies are due to the predominance of the species such as Fe^{2+} ions, interfacial dislocations piles-up, oxygen vacancies, grain boundary effects etc. [12]. For our material Fe^{3+} ion is the predominant ion, in which the electronic exchange between neighbors takes place.

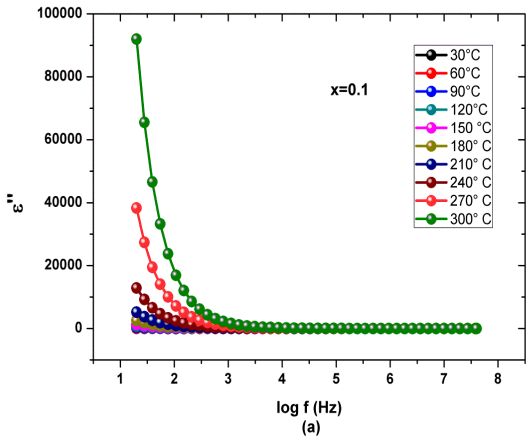

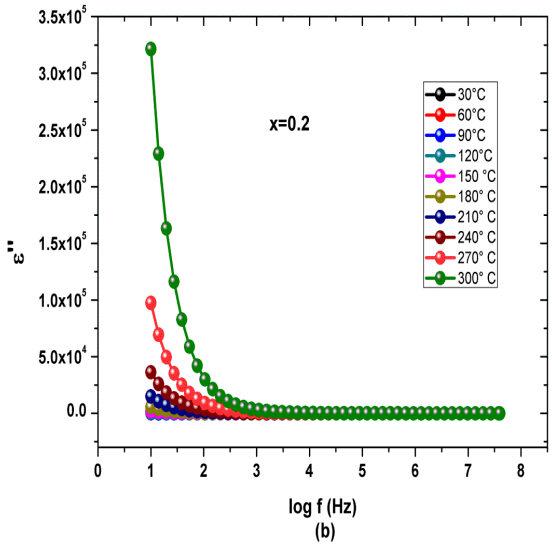

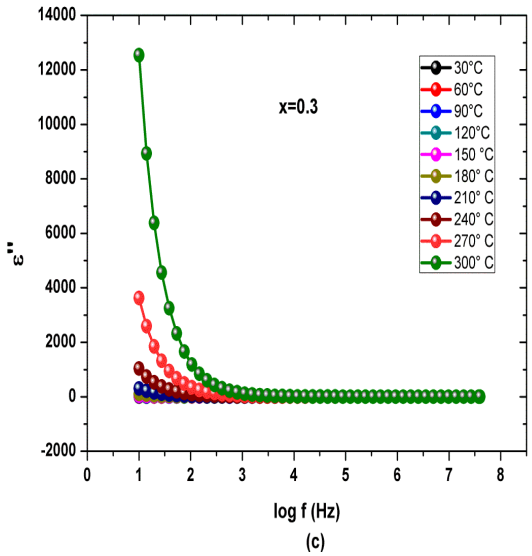

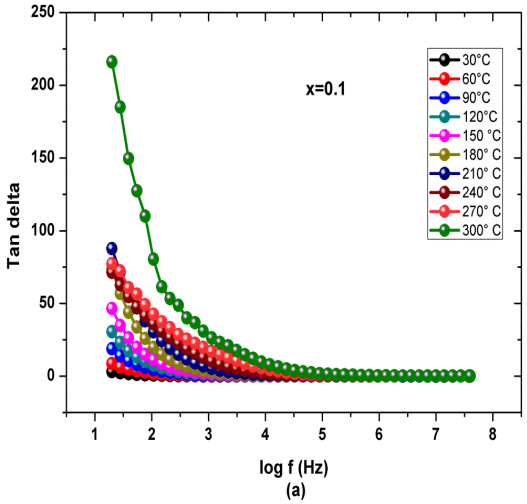

Figure.3 (a-c) Variation of imaginary part of dielectric permittivity (ε'') with frequency of $SrFe_{12-x}Ag_xO_{19}$ (x=0.1, 0.2, 0.3) at different temperatures

Dielectric loss tangent in ferrites represents the total core loss in the material. Low core loss requires low dielectric losses. The value of tangent loss is dependent on the stoichiometry, Fe^{2+} contents and structural homogeneity and the sintering temperature of the samples [13]. The variation of loss tangent with frequency can be observed from the Figure.5.

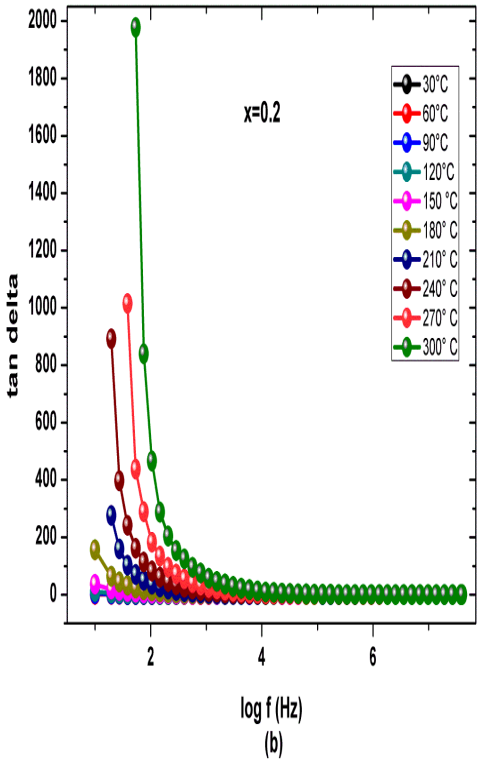

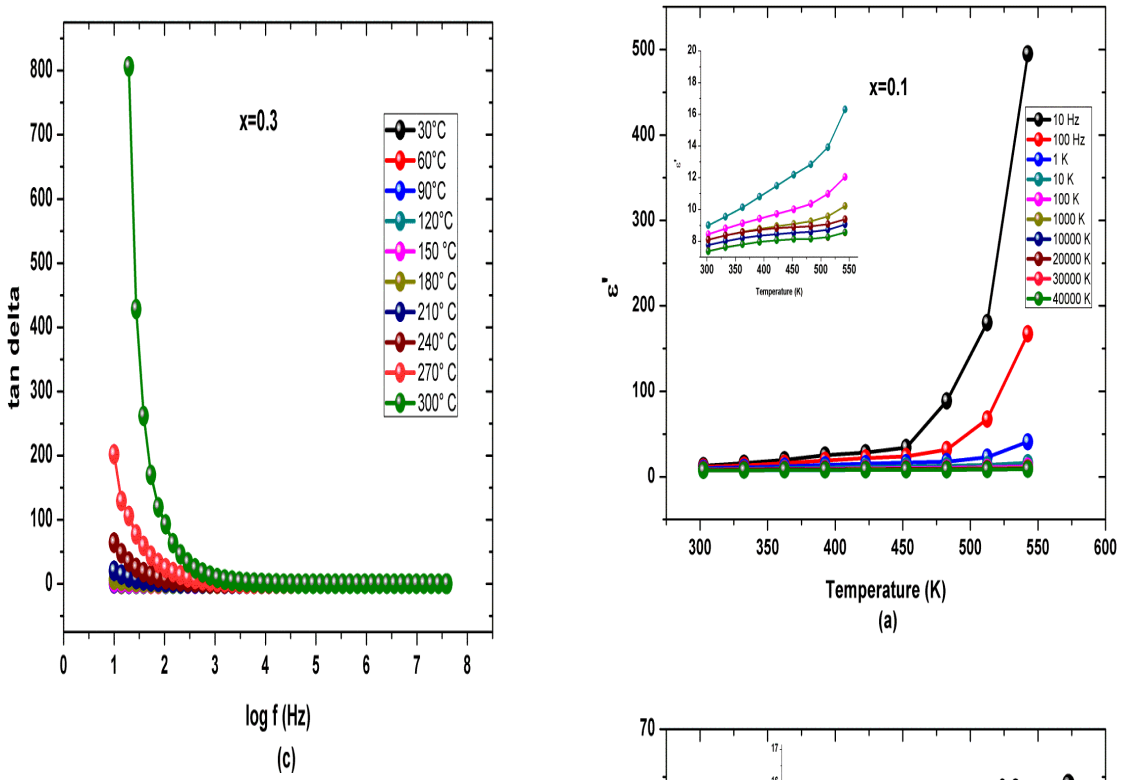

Figure.4 (a-c) Variation of loss tangent (tan δ) with frequency of $SrFe_{12-x}Ag_xO_{19}$ (x=0.1, 0.2, 0.3) at different temperatures

4.3.2. Variation of Dielectric constant and Tangent loss with temperature

Figure.5 (a-c) shows the variation of dielectric constant with temperature for the $SrAg_{(1-x)}Fe_{(12-x)}O_{19}$ (x=0.1, 0.2, 0.3). It can be seen that ε' increases with temperature up to 450°C which is around the curie temperature (T_c) of ferrites. This change in ε' is due to the magnetic transition of ferrites from ferromagnetic to paramagnetic phase at T_c. This may be due to the hopping of electrons between Fe^{2+} and Fe^{3+} ions induces dielectric polarization in ferrite samples which in turn increases ε'. The dielectric constant found to increase symmetrically with the increase in temperature due to polarization.

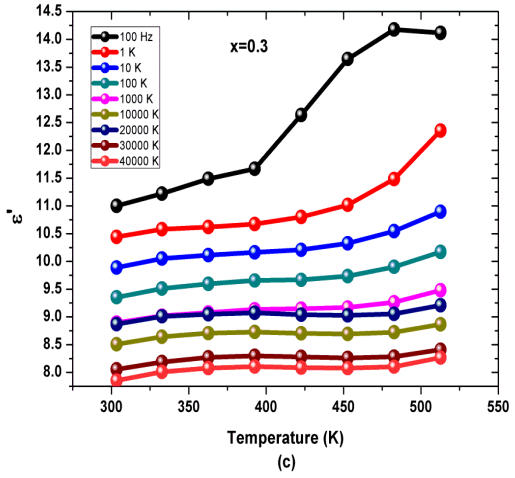

Figure.5 (a-c) Variation of dielectric constant (ε) with temperature of $SrFe_{12-x}Ag_xO_{19}$(x=0.1, 0.2, 0.3) at different frequencies

The dielectric loss (tan δ) is the energy loss observed within the material during conduction of electrons. Hopping of electrons produces polarization which changes with respect to applied field. Figures.7 (a-c) shows the variation of tan δ at constant frequency for different selected temperatures. By increasing the temperature, the electrons and ions get thermally activated, increases the conduction and hence there is an increase in the value of tan δ. temperature.

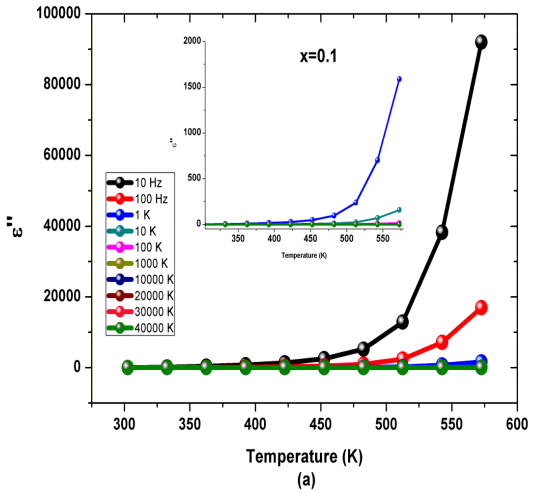

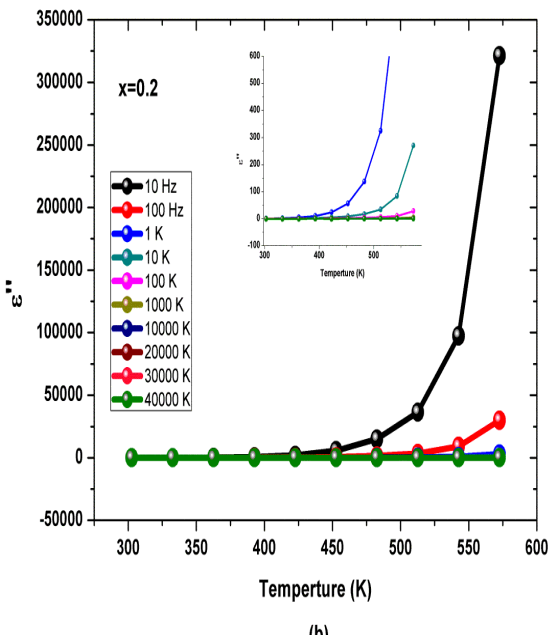

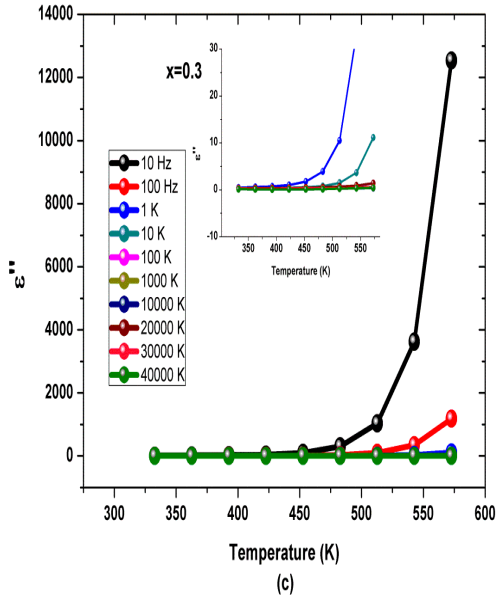

Figure.6 (a-c) Variation of loss tangent (tan δ) with temperature of $SrFe_{12-x}Ag_xO_{19}$(x=0.1, 0.2, 0.3) at different frequencies

Figure 7 (a-c) shows the variation of AC conductivity with temperature of $SrAg_xFe_{12-x}O_{19}$ (x=0.1, 0.2, 0.3) at different selected frequencies. The ac conductivity caused by the hopping processes at the

octahedral site and is a frequency dependent. The conduction mechanism in ferrites is due to the hopping of charge carriers between the Fe ions at octahedral sites. The increase of conductivity with temperature is due to increase in the mobility of charge carriers. The conductivity increases with increasing temperature and also increases with increasing the Ag content as a function of frequency. According to Maxwell-Wagner model, at low frequencies the ac conductivity is due to the grain boundary behavior and at high frequencies, it is attributed to the grains at which the material acts as a good conductor and also there is an increase in hopping of electrons between Fe^{3+} and Fe^{2+} ions which increases conductivity.

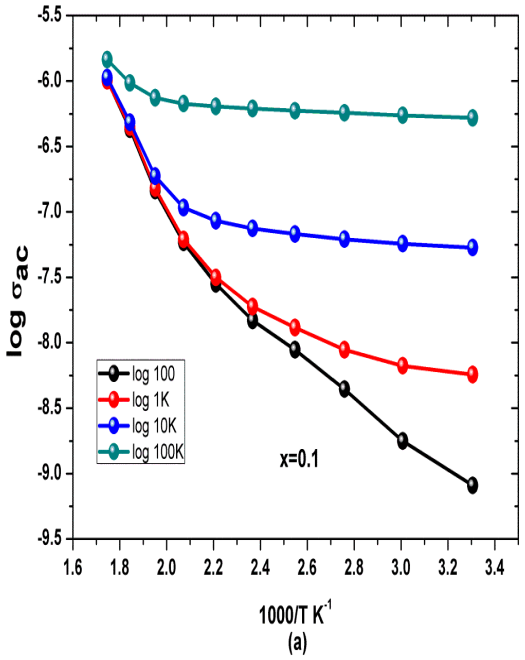

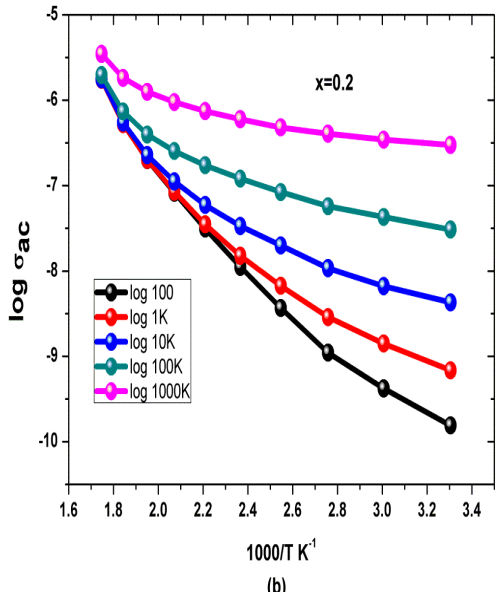

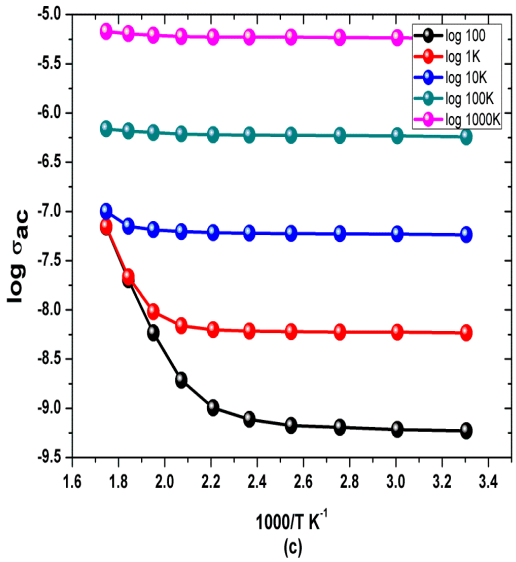

Figure.7 (a-c) Variation of ac conductivity (σ_{ac}) with temperature of $SrFe_{12-x}Ag_xO_{19}$(x=0.1, 0.2, 0.3) at different frequencies

5. CONCLUSION

The hexagonal single phase materials of $SrFe_{12-x}Ag_xO_{19}$ (x=0.1, 0.2 and 0.3) system were successfully prepared by sol-gel route. Structural characterization by powder X-ray diffraction study confirms

the hexagonal phase of the samples. From the structural analysis it was found that at high Ag doping level, metallic silver is formed as secondary phase. The higher doping of Ag in $SrFe_{12}O_{19}$ showed lowest dielectric permittivity and dielectric loss. The conductivity of the as prepared composites increases with increasing the Ag^{1+} content as a function of frequency and temperature.

REFERENCES

1. OKASCHA, A. Spectroscopic Analyses of the Photocatalytic Behavior of Nano Titanium Dioxide. Spectrochimica Acta Part A: Molecular And Biomolecular Spectroscopy.136,2015,504-509

2. .Dursun, S. et al. Comparison of the structural and magnetic properties of submicron barium hexaferrite powders prepared by molten salt and solid state calcination routes. *Ceramics International*, 38(5), 2012 pp.3801–3806.

3. Thakur, A., Singh, R.R. & Barman, P.B., Crystallization Kinetics of Strontium Hexaferrite : Correlation to Structural , Morphological , Dielectric and Magnetic Properties. , 8(6), 2012pp.595–603.

4. Liu, X. et al., 2012. Magneto-optical Kerr spectra and magnetic properties of Co-substituted M-type strontium ferrites. *Materials Chemistry and Physics*, 133(2–3), pp.961–964.

5. Haq, A. & Anis-ur-rehman, M., 2012. Effect of Pb on structural and magnetic properties of Ba-hexaferrite. *Physica B: Physics of Condensed Matter*, 407(5), pp.822–826.

6. Online, V.A. et al., 2013. induce multiple photoluminescence and room. , pp.1885–1895.

7. Thankachan, S. et al., 2014. Effect of rare earth doping on structural , magnetic , electrical properties of magnesium ferrite and its catalytic activity. , 3(4), pp.529–537.

8. Chawla, S.K. et al., 2014. Sol–gel synthesis, structural and magnetic properties of nanoscale M-type barium hexaferrites BaCoxZrxFe(12−2x)O19. *Journal of Magnetism and Magnetic Materials*, 350, pp.23–29.

9. Salamati, A.P.P.K.H., 2013. Structural , magnetic and electromagnetic wave absorption properties of SrFe 12 O 19 / ZnO nanocomposites. , pp.186–191.

10. Javed Iqbal, M., Naeem Ashiq, M. & Hussain Gul, I., 2010. Physical, electrical and dielectric properties of Ca-substituted strontium hexaferrite (SrFe 12O 19) nanoparticles synthesized by co-precipitation method. *Journal of Magnetism and Magnetic Materials*, 322(13), pp.1720–1726.

11. Mohamed, M., Wahba, A. & Yehia, M., 2014. Structural and magnetic properties of CoFe 2− x Mo x O 4 nanocrystalline ferrites. *Materials Science and Engineering: B*, 190(1), pp.52–58.

12. Wagner, T.R., 1998. Preparation and Crystal Structure Analysis of Magnetoplumbite-Type BaGa 12 O 19. , 124(136), pp.120–124.

Ghzaiel, T. Ben et al., 2016. Effect of non-magnetic and magnetic trivalent ion substitutions on BaM-ferrite properties synthesized by hydrothermal method Jl.of Alloys and compounds 671,2